# Inverse Iterative Methodology for Welded Joints Characterization in Construction Designing and Comparison to Classical Approach

**Ana Petrovic[1], Nikola Momcilovic[1], Branislav Djordjevic[2], Simon Sedmak[2], Nina Andjelic[1], Radomir Jovicic[2], Mihajlo Arandjelovic[2]**

[1] University of Belgrade, Faculty of Mechanical Engineering, Kraljice Marije 16, 11120 Belgrade, Serbia
aspetrovic@mas.bg.ac.rs, nmomcilovic@mas.bg.ac.rs, nandjelic@mas.bg.ac.rs

[2] Innovation Centre of Faculty of Mechanical Engineering, Kraljice Marije 16, 11120 Belgrade, Serbia
brdjordjevic@mas.bg.ac.rs, ssedmak@mas.bg.ac.rs, rjovicic@mas.bg.ac.rs, msarandjelovic@mas.bg.ac.rs

*Abstract: Traditional approach in structural designing and strength assessment that observes structure without welded joints is sufficiently accurate in terms of elastic response, in comparison to yield strength. The main idea of this paper is to show that it is necessary to consider welded joints and all their regions in the elastic-plastic domain. This methodology proposes obtaining of mechanical properties of welded joint regions using inverse iterative procedure developed by the authors of this paper. Taking into account tensile testing of specimens containing welded joints, strain field was obtained using Digital Image Correlation. Finite Element Method model of test specimens is formed using the same parameters as in the experimental one (such as welded joint geometry, boundary conditions, loads, etc.). Strain fields of all regions of welded joint (parent material, weld metal, and heat affected zone) are imported into finite element model, setting ground for development a new, improved, finite element model. Consequently, material properties of all three welded joint regions were obtained. Demonstration of the proposed procedure is shown in the analysis of two significant structures: (i) a pipeline (membrane stress), and (ii) a girder of a bucket wheel excavator (bending of plates). Based on this analysis it was shown within the plastic deformation domain the differences in stresses (and structural behavior in overall) between structure with and without welded joints are considerable, while there is no difference in the elastic domain. Stress concentration factors are formulated for each analyzed type of structure, in order to quantify those differences.*

*Keywords: welded joint; finite element method; digital image correlation; inverse iterative methodology; stress concentration factor*

**List of abbreviations**

DIC – digital image correlation
FE – finite element
FEA – finite element analysis
FEM - finite element method
HAZ – heat affected zone
IIM – inverse iterative methodology
MAG - metal active gas
WM – weld metal

# 1 Introduction

In the case of large steel structures [1-3], traditional approach in designing and structural integrity assessment includes the finite element method (FEM) analysis [4-6] that considers structural elements and their effect on rigidity and strength (without welded joints) [7-9], as can be seen in numerous papers [10-13]. In papers [2-4] analysis of bucket wheel excavator structural parts was performed, including slewing platforms and bogeys. Papers [6-8] deal with other structural parts such as undercarriage supports and chain links. Some of the papers, namely [4, 10, 11] focus on a specific type of bucket wheel excavators, the SchRs630. Welded joints were not taken into account in those finite element analyses (FEA), despite being inevitable parts of large steel structures.

There are many papers in which the experimental testing of a structure part containing welded joint was performed but few of them include FEA of welded joints and welded joint region properties. In paper [14] experimental investigation on cold-formed steel elliptical hollow section T-joints is performed, with disregarding welded joints properties in FEA. Similar analysis of a girder (containing welded joints) was performed in paper [15]. In paper [16] experimental testing of a structure containing welded joints was performed without using FEA. On the other hand, paper [17] included FEA which was performed without considering welded joints, but its authors proposed a method for improvements of FEM with the purpose of obtaining the same deformation in FEA and the experiment.

Unlike the traditional designing approach that is based on the yield strength as the highest limit, modern approach recognizes the ultimate strength as highest limit in structural analysis. In that kind of design, sudden overloading that leads to structural collapse is covered. The ultimate strength of structure is a subject of discussion in recent papers, such as [18-20]. In paper [18], compressive strength of a part (containing welded joints) of a transmission tower is tested using numerical-experimental approach. In paper [19] ultimate strength of gusset plate joints with ring stiffener plates under tension was calculated. In both papers, FEA included holes and screws without considering the existence of welded joints. In paper [20] strength of stiffened welded tubular joints in floating energy production structures is tested. In this case, FEM contained welded joint as a radius between two cylindrical parts to eliminate stress concentration, without considering mechanical properties of welded joints in general. In paper [21], all regions of welded joint properties were considered to have the same as material properties as the filler material. Papers [22, 23] reported 16% to 32% reductions in the ultimate strengths of S960 steel grade parent materials around the welds. In both papers tensile testing of specimen was performed, while deformation field was obtained using DIC. From aforementioned it can be concluded that is important to consider welded joints and properties of their regions.

Papers [24, 25] considered differences of material properties of parent material and weld metal (WM), while heat affected zone (HAZ) properties are neglected in FEA, with highlighting the importance of weldment failures with potentially catastrophic consequences.

Two specific ways of considering welded joints are given in papers [26, 27]. The deformation capacity of the welded connection was measured via a non-contact process using the DIC technique in [26]. Based on these results, inclined shell element with rigid links was used to accurately represent the geometry and rigidity of fillet welds and was formulated for the case of bending of welded structure. In paper [27] numerical modelling of welded T-joint configurations using SYSWELD was presented. Unlike the previous two papers, methodology that will be presented in this research does not need any other resources besides program based on FEM. Also, it gives a simple solution that takes into account different material properties in the elements in the vicinity of welded joints.

Significance of knowing of mechanical properties of new materials is highlighted in papers [28-31]. In papers [29, 30], the focus was on determining the mechanical properties of the HAZ, along with measuring of hardness. Paper [32] also deals with material characterisation for new applications, and demonstrates its use on non-metallic materials.

Membrane stresses are based on different calculation philosophy, even simpler than the bending one. Despite that, pipelines represent structures of high importance as highlighted in paper [33]. Statistical analysis of accidents data on hazardous materials pipeline failures has been carried out to identify the most common causes and consequences of failures. In paper [34], it is stated that 8.7% of pipeline incidents since 2005 were caused by material failure of pipe or weld.

The main idea of this paper is to give the alternative solution to traditional approach that observes structure without welded joints. Authors of this paper proposed a methodology for characterization of all welded joint regions based on experimentally obtained strain fields and FEM, with the aim of formulation of an improved FE model of welded joints. Two types of structure were selected to demonstrate the significance of adequate welded joints properties. The first structure to be analyzed is a pipeline loaded with internal pressure causing membrane stresses. Then, the girder of bucket-wheel excavator is analyzed, with the shape of standard I profile and exposed to bending for most of its exploitation period. In both cases, structural analysis was performed with and without welded joints, including material properties of all three welded joint regions. Universal conclusions based on type of loading (membrane and bending) were formulated in the form of stress concentration factors.

# 2 Method

## 2.1 Inverse Iterative Methodology

This subchapter will present the inverse iterative methodology (IIM) for obtaining mechanical properties of welded joint regions developed by authors of this paper. This methodology included development of a new improved finite element (FE) model based on strain field obtained from the experiment. For that purpose, tensile testing of several specimens containing welded joints was performed.

Specimens are made of steel of commercial designation S275JR (EN 1.0044 according to standard EN 10025-2: 2004 Hot rolled products of structural steels. Technical delivery conditions for non-alloy structural steels) using manual arc welding (MAG) process with overmatching effect since the filler material used for welding is VAC 60 wire (standard designation G42 5M/C G3Si1 according to EN ISO 14341-A), manufacturer of Železarna Jesenice. Mechanical properties of aforementioned steel S275JR and pure weld of used filler material are given in Table 1.

Table 1
Mechanical properties of S275JR (parent material) and pure WM made of VAC 60

| Material | **Yield strength [MPa]** | **Tensile strength [MPa]** | **Deformation [%]** |
|---|---|---|---|
| S275JR (*parent material*) | > 275 | 410-560 | |
| VAC 60 (*pure weld metal*) | > 410 | 510-590 | > 22 |

Four different groups of specimens were tested, with three samples from each group, with a thorough explanation given in [35].

During the tensile testing, strain field was continuously measured using stereo cameras, and results were processed using the Aramis system, based on DIC [36, 37]. This method is based on comparison of photographies in undeformed and deformed stage, in such a way that point displacements are measured continuously during tensile testing, while deformations (strain fields) are computed. Surface which will be recorded needs to be adequately prepared, in terms of cleaning and painting [38]. It should be noted that the use of DIC in this research was relatively simple, since the material and dimensions of specimens were selected in a way that avoided issues which can occur with very thin specimens/sheets.

As a result of experimental testing, the whole strain field is obtained in all stages of loading. Of all those stages, the most interesting one is the moment when plastic deformation begins to occur.

FEM represents a very powerful tool used mostly for loading analysis [39-41], with main purposes of obtaining stress distribution fields, strain distribution, investigating of 'critical' spots in a structure, etc. In this particular case, FE models of test specimens were formed using the same parameters as the experiment (welded joint geometry, boundary conditions, loads, etc.). Since the force is measured at the moment when plastic deformation occurs, it was possible to formulate initial FE models with its boundary conditions and loads, shown in Fig. 1.

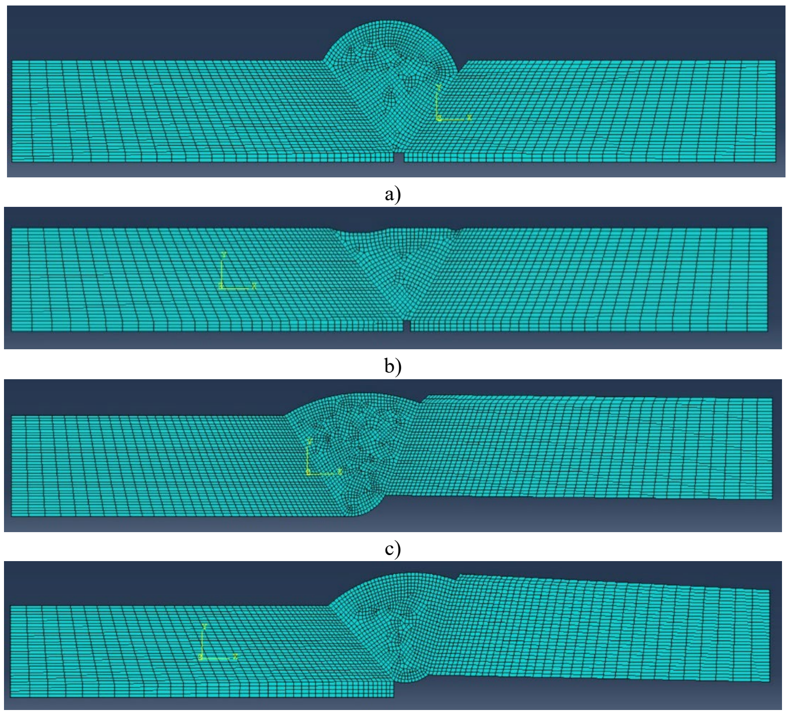

a)

b)

c)

d)

Figure 1

FE model of four different specimen group with welded joints and: a) Excess WM / undercut / incomplete root penetration as defects; b) WM sagging / incomplete root penetration as defects; c) Excess WM / undercut / misalignment as defects; d) Undercut / misalignment / incomplete root penetration as defects

In all these initial models, material properties of all three welded joint regions (parent material, WM and HAZ) were assumed. Properties of the parent material and pure WM were shown in Table 1, while HAZ properties were unknown. To improve the FE models, deformations of all regions of the welded joint are iteratively imported into initial models. They were determined until the strain field obtained by FEA converged to the strain field obtained by experimental testing.

HAZ is treated as a sub-area of the welded joint whose mechanical properties needed to be evaluated. HAZ is considered one region due to the metallurgical properties of the parent material since there was no need for subdivision of this specific area. Therefore, there is no expectation of grain size difference in HAZ. Microscope examination confirmed the uniformity of HAZ structure, along with its assumed properties.

Because of the nature of the problem, one more step is included, as can be seen in the algorithm in Fig. 2. That is the step during which other potnetial causes of failure should be considered, besides mechanical properties of welded joint regions, which could lead to differences in strain field between FE model and measured strain field by experiment. This particular case occurred in one of the specimens which will be discussed in the next chapter.

Consequently, the results of this procedure are the material properties of all three welded joint regions. Also, stress causing plastic deformation was computed.

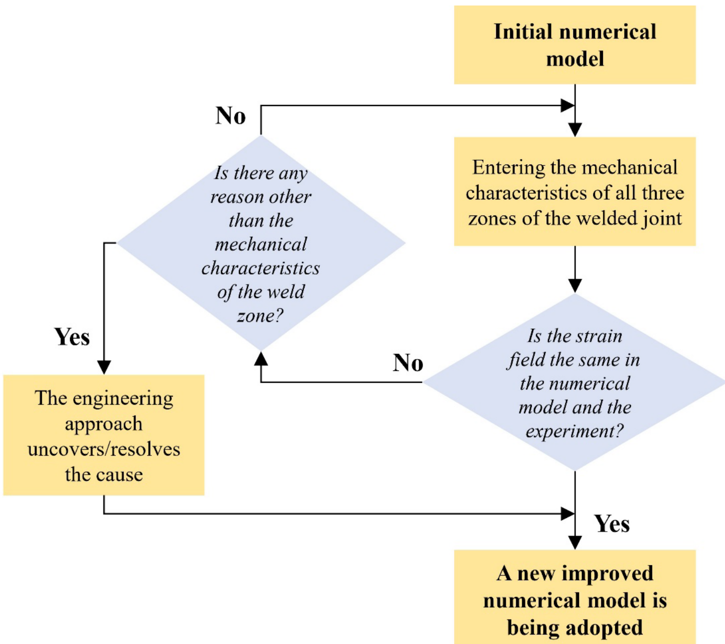


Figure 2
Algorithm of inverse iterative methodology (IIM)

## 2.2 FE Models for Pipeline and Beam (girder) containing Welded Joints

Firstly, information about material properties of all three welded joint regions is used in analysis of welded joint influence to structural integrity of a pipeline structure. A pipeline structure is chosen for demonstration of this methodology application since it is loaded with internal pressure, and the stresses are mostly membrane. Three FE models were developed. The first one (FEM 1) represents the simplest case, i.e. the case without a welded joint, representing the traditional approach to structural strength (linear-elastic computational analysis), illustrated in Fig. 3.

Pipeline FE model with welded joints is illustrated in Fig. 3b. This model was used for two FEAs: (i) FEM 2, with HAZ that has the same properties as the parent material, (ii) FEM 3, in which properties of all three welded joint regions were taken into account.

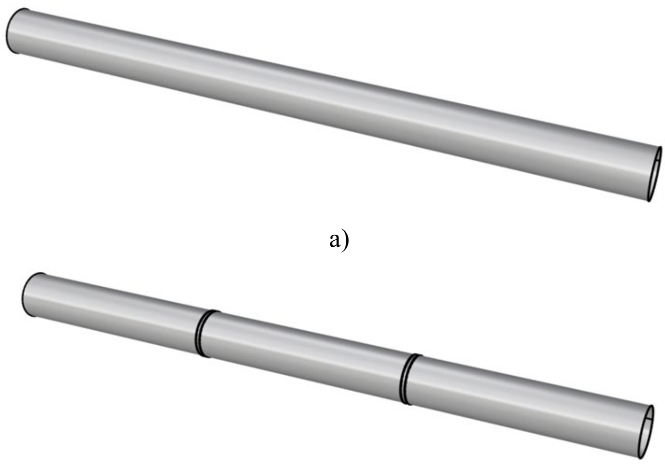

b)

Figure 3

FE models of pipeline a) without welded joints b) with welded joints

Pipeline diameter is 108 mm, with thickness of 12 mm, and pipeline segment length (between two welded joints) of 500 mm. Pipe wall thickness is in accordance with the experimentally measured specimen thickness. Pipeline was modeled using thin shell elements (Fig. 4), and classical plate theory was applied. The size of welded joint regions is the average value of the zone size of tested specimens. Weld metal region is 7 mm wide, with HAZ which was 2.5 mm wide, positioned on both sides of WM.

The ends of a pipe are clamped, displacement and rotation of all points (in the whole circumference) are suppressed. The pipe is loaded with internal pressure.

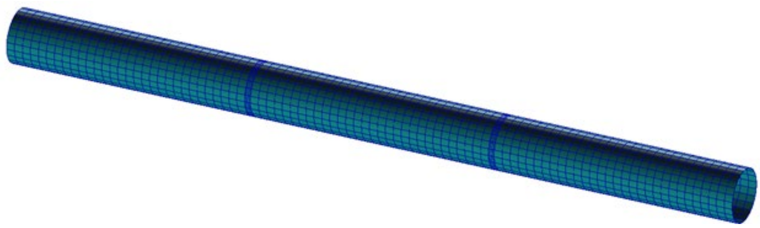

Figure 4
FE model of pipeline, shell elements

Similar to pipeline model, three FE models of girder are developed. FE model with plate elements is shown in Fig. 5a. Weld metal region is 5 mm wide, with HAZ of 2.5 mm wide positioned from both sides of WM (Fig. 5b). Vertical plate thickness is 12.2 mm and horizontal plate thickness is 18.3 mm as in standard I 34 profile considering specimen thickness of 12 mm. Girder was modeled using thin plate elements, applying classical plate theory.

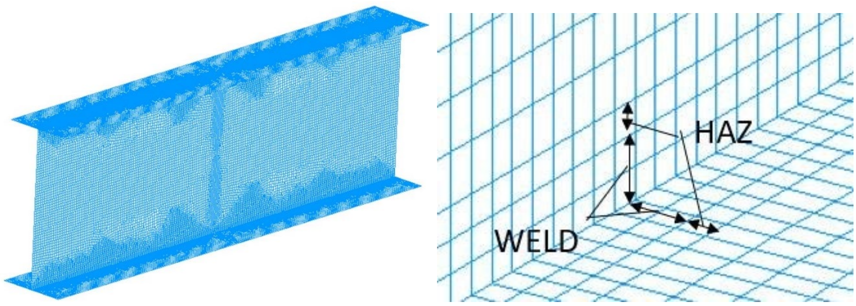


a) b)

Figure 5
FE model of I profile shape girder, a) plate elements; b) zone dimensions

# 3 Results

## 3.1 Inverse Iterative Methodology Application

Fig. 6 shows the strain field in the moment when plastic deformation occurs, obtained using DIC and improved FEA for all four different specimen groups. In case of the third specimen, lack of fusion during welding process occurred in the real specimen.

One more step is added into IIM which included engineering assessment of the cause of the difference in strain field between FE model and measured strain field, besides mechanical properties of welded joint regions. When lack of fusion is taken into account and FE model is adjusted, the strain fields becomes the same (Fig. 6 case 3). New improved FE models are shown in Fig. 6 (on the right side) for each specimen.

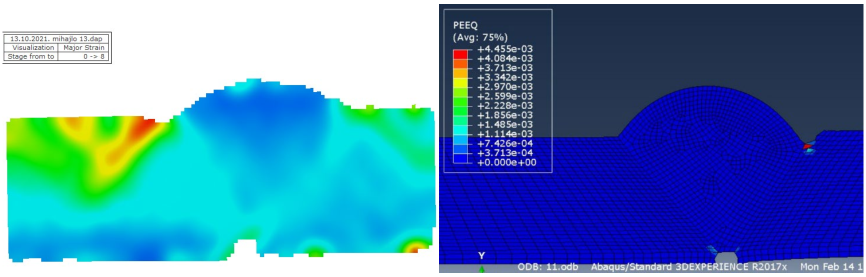


1st group specimen - strain field: left) obtained by DIC; right) FEA

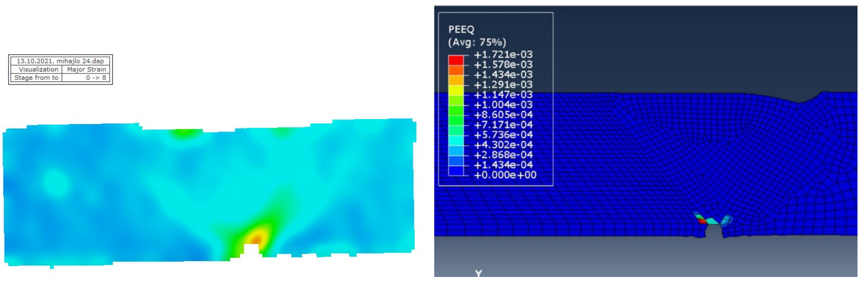


2nd group specimen - strain field: left) obtained by DIC; right) FEA

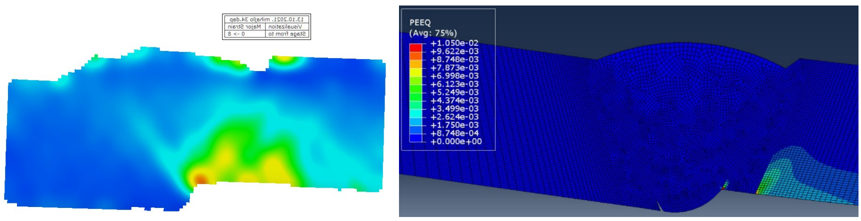


3rd group specimen - strain field: left) obtained by DIC; right) FEA

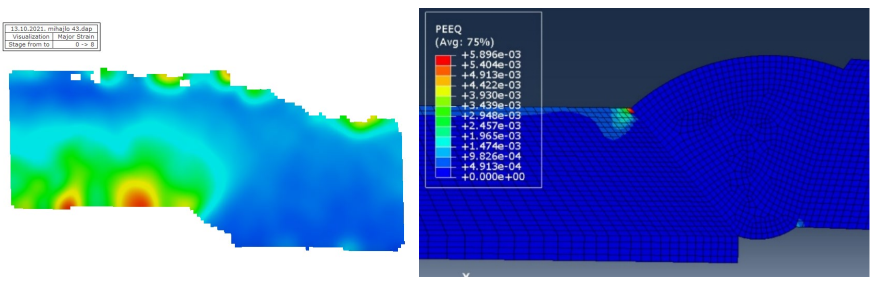


4th group specimen - strain field: left) obtained by DIC; right) FEA

Figure 6

Strain filed obtained using Aramis system and improved numerical computational model for all four specimen groups, in a moment when plastic deformation occurs

As explained, material properties of all three welded joint regions were obtained and stress causing plastic deformation is computed. Material properties of parent material and WM are in accordance with values given in Table 1. This could be treated as first verification of this methodology, and it is indirect confirmation that the HAZ properties values are evaluated properly. Mechanical properties of HAZ, for all five specimen groups, obtained by IIM are shown in Table 2.

Table 2
Material properties of HAZ obtained by IIM

| **Specimen group** | **Yield strength [MPa]** | **Tensile strength [MPa]** | **Deformation [/]** |
|---|---|---|---|
| *Group 1* | 404 | 497 | 0.055 |
| *Group 2* | 395 | 505 | 0.06 |
| *Group 3* | 419 | 495 | 0.06 |
| *Group 4* | 390 | 484 | 0.055 |

It could be observed that properties of HAZ are closer to WM properties than parent material, which was the assumption in the beginning of this research. Considering deformation levels of 5.5% - 6% when plastic deformation occurs, their values are lower than in the parent material, which is also expected considering that (by engineering experience) HAZ has a lower capacity of plasticity than the parent material. From the previous table can be seen that yield strength values are in a range from 390 MPa to 419 MPa, while tensile strength values are in a range from 484 MPa to 505 MPa.

Obtained values that will be used in further calculations are shown in Table 3. For material properties approximate average values are adopted as referent values.

Table 3
Material properties of all three welded joint regions obtained using IIM

| **Welded joint region** | **Yield strength [MPa]** | **Tensile strength [MPa]** |
|---|---|---|
| *Parent material* | 275 | 440 |
| *WM* | 460 | 600 |
| *HAZ* | 400 | 495 |

Material properties used in further FEA are illustrated in Figure 7. In FEAs bilinear curve is used for plasticity, while in the Fig. 7 plasticity domain is illustrated as a straight line.

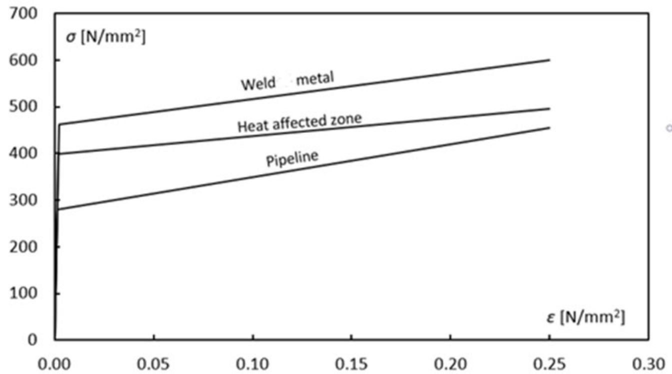


Figure 7

Illustration of material properties obtained using IIM

## 3.2 Structure with Membrane Stress

As previously said, three FE models were developed. The first one is without a welded joint, the second and the third pipeline included the welded joint. In the second one, HAZ had the same properties as the parent material, although it is proven that its properties are closer to properties of the WM. In the third one, special attention is paid to HAZ properties. Material properties of all three regions obtained using IIM were taken into account.

As far as linear elastic analysis was considered, all three FEA gave the same results. Firstly, linear elastic analysis was performed. Model of the pipe is clamped in the ends and loaded with internal pressure, causing membrane stress in the structure. Von Mises stress results of linear elastic computations for pipe containing welded joints are given in Fig. 8, for the pressure value of 10 MPa.

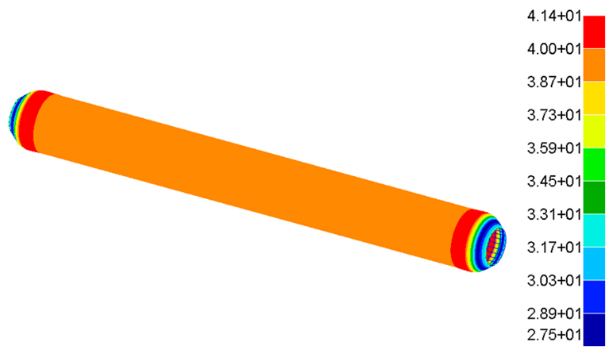


Figure 8

Von Mises stress in [MPa] for linear elastic analysis of the pipeline containing welded joints loaded with internal pressure p = 10 MPa

Results are the same (there is no stress concentration in the zone of welded joints), as in the case of pipe without welded joints. In that way, it was proven that considering linear elastic analysis existence of welded joint could be neglected, and FEA could be performed without welded joints, in a case of pipeline loaded with internal pressure (causing membrane stress in the material). An explanation is simple - from diagram in Figure 7, it can be seen that Young's modulus of elasticity for all three materials (parent material, WM, HAZ) is practically the same.

Non-linear computation in plastic domain was performed for all three models. Start of the plastic deformation for the first FE model is shown in Fig. 9.

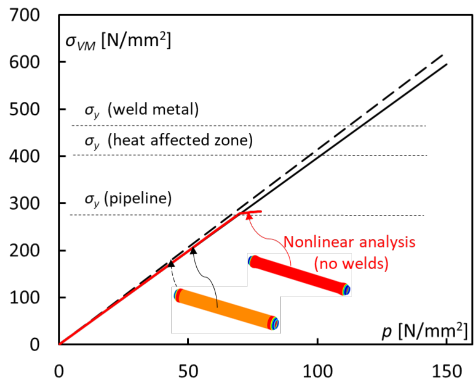


Figure 9

Nonlinear analysis: the first FE model of the pipeline (without welded joints)

The third FE model behavior in plastic domain is shown in Fig. 10.

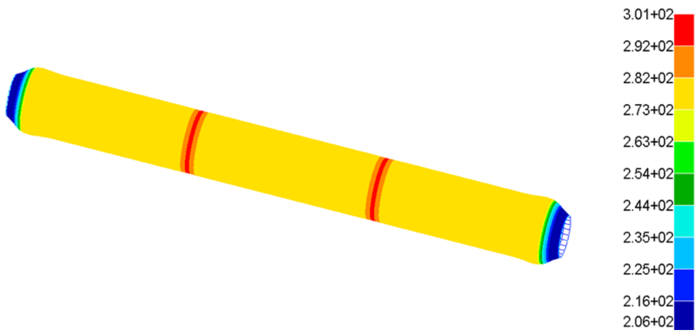


Figure 10

Von Misses stress [MPa] for nonlinear analysis of the third model of the pipeline loaded with internal pressure p = 73 MPa

Stress results in the zone of welded joints for the second and the third FE model are shown in Table 4.

Table 4
Non-linear analysis (plastic domain) of the pipeline

| | Internal pressure [MPa] | Stress in the zone of parent material [MPa] | Stress in HAZ [MPa] | Stress in WM [MPa] | Stress concentration factor [/] |
|---|---|---|---|---|---|
| The second model (*HAZ = parent material*) | 77 | 285 | 326 | 454 | 1.59 |
| The third model | 77 | 282 | 373 | 416 | 1.47 |

Stress concentration factors are shown in the last column. As one can notice, stress concentration factor decreased when HAZ real properties were included into the calculation. It can also be seen that the stress gradient in the zone of welded joint is completely different in these two cases, implying the significance of HAZ region properties.

## 3.3 Structure with Bending and Sheer Stress

As previously said, three FE models were developed for this analysis as well. The first one is without a welded joint, the second and the third pipeline included welded joints. In the second analysis, HAZ had the same properties as the parent material. As far as linear elastic analysis was considered, the same as in case of a pipe, all three FEAs gave the same results. Von Mises stress for girder containing welded joints is shown in Fig. 11. Total force applied is 147 060 N, and is linearly distributed in mesh knots at half of the beam span. Results suggest that there is no difference in stress field in all three models for this particular structure as well. In that way it was proven that, considering linear elastic analysis, existence of welded joint could be neglected as it does not affect the stress distribution, hence FEA could be performed without welded joints as well.

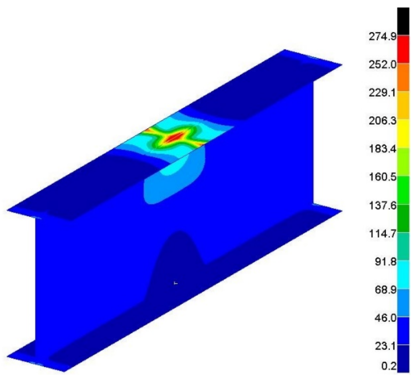


Figure 11
Von Mises stress [MPa] for linear elastic analysis of the girder containing welded joints loaded with F= 147 060 N

The first FE model behavior in the plastic domain is shown in Fig. 12.

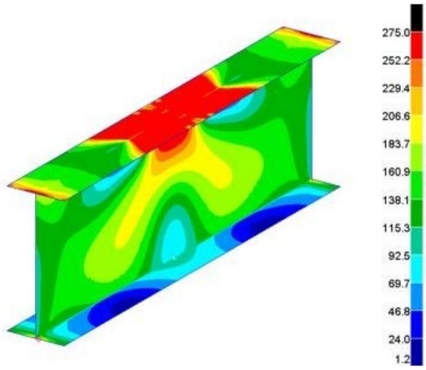


Figure 12
Von Mises stress [MPa] for nonlinear analysis of the first model of the girder loaded with F = 570 000 N

Stress results in the zone of welded joints for the first FE model are shown in Table 5.

Table 5
Nonlinear analysis (plastic domain) of the girder - the first model

| | Applied force [N] | Stress in the zone of parent material [MPa] | Stress in HAZ [MPa] | Stress in WM [MPa] | Stress concentration factor $S_F$ [/] |
|---|---|---|---|---|---|
| The first model | 570 000 | 170 | 274 | 274 | 1.61 |

The behavior in plastic domain of the second and the third computational model is shown in Fig. 13.

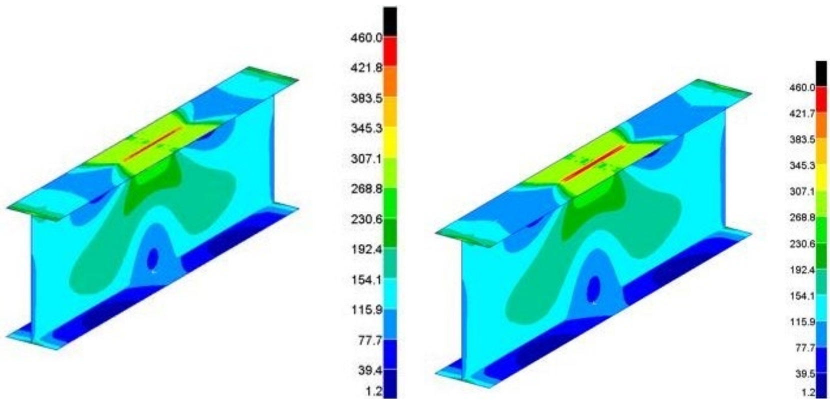


Figure 13
Von Mises stress [MPa] for nonlinear analysis of the a) second and a) the third model of the girder, loaded with $F$ = 570 000 N

As can be seen from Figs. 12 and 13, stress distribution field appearance is different when the structure is observed without welded joint and when it contains welded joints. The reason lies in the fact that the welded joint, being the locally ‘strongest’ part of the structure taking into account overmatching effect, bears the most of the loading force. Stress results in the zone of welded joints for the second and the third FE models are shown in Table 6.

Table 6

Non-linear analysis (plastic domain) of the girder: the second and the third model

| | **Applied force [N]** | **Stress in the zone of parent material [MPa]** | **Stress in HAZ [MPa]** | **Stress in WM [MPa]** | **Stress concentration factor *S* [/]** |
|---|---|---|---|---|---|
| The second model (*HAZ = parent material*) | 570 000 | 170 | 320 | 440 | 2.59 |
| The third model | 570 000 | 170 | 390 | 450 | 2.65 |

Stress concentration factor in case of girder should be estimated as follows. Considering Table 5, stress concentration factor is the consequence of loading, is the highest in section in which the bending moment is the highest. In table 6 stress concentration factor is a consequence of force being applied and the existence of welded joint, as shown in Eq. (1):

$$S = S_F \cdot S_{WJ} \tag{1}$$

In case of the third model stress concentration factor could be determined as Eq. (2):

$$S_{WJ} = \frac{S}{S_F} = \frac{2.65}{1.61} = 1.64 \tag{2}$$

The general remark is that stress concentration factor in the zone of welded joint is 1.5 for shell and plate elements loaded with internal pressure, and 1.65 for beam elements loaded with bending forces.

## Conclusion

Based on the methodology presented in this paper, following conclusions can be drawn:

- Developed IIM was shown to be appropriate for assessment of all welded joint regions mechanical properties, including the HAZ. One of the products of IIM is a new and improved FE model of welded joints.
- HAZ properties can be determined using proposed IIM.
- It was proven that in plastic domain, mechanical properties of all welded joint regions (particularly HAZ) must be included in FEA, which can be obtained by applying proposed methodology.

- For shell and plate elements loaded with internal pressure, stress concentration factor in the zone of welded joint equals 1.5, while for beam elements loaded with bending forces equals 1.65.

**Acknowledgement**

Authors of this paper would like to express their gratitude to the Ministry of Education, Science and Technological Development, Republic of Serbia, Grant no 451-03-47/2023-01/200105. and 451-03-66/2024-03/ 200213 from 05.02.2024., for supporting our work.

**References**

[1] Motok M., Momčilović N., Rudaković S.: Reliability based structural design of river–sea tankers: Still water loading effects, Marine Structures, Vol. 83, 2022, 103202

[2] Bošnjak S., Petković Z., Zrnić N., Simić G., Simonović A.: Cracks, repair and reconstruction of bucket wheel excavator slewing platform, Engineering Failure Analysis, Vol. 16, 2009, pp. 1631-1642

[3] Bošnjak S., Petković Z., Zrnić N., Pantelić M., Obradović A.: Failure analysis and redesign of the bucket wheel excavator two-wheel bogie, Engineering Failure Analysis, Vol. 17, 2010, pp. 473-485

[4] Bošnjak S., Pantelić M., Zrnić N., Gnjatović N., Đorđević M.: Failure analysis and reconstruction design of the slewing platform mantle of the bucket wheel excavator O&K SchRs 630, Engineering Failure Analysis, Vol. 18(2), 2011, pp. 658-669

[5] Trifković D., Stupar S., Bošnjak S., Milovančević M., Krstić B., Rajić Z. Dunjić M.: Failure analysis of the combat jet aircraft rudder shaft, Engineering Failure Analysis, Vol. 18(8), 2011, pp. 1998-2007

[6] Bošnjak S., Petković Z., Simonović A., Zrnić N., Gnjatović N.: 'Designing-in' failures and redesign of bucket wheel excavator undercarriage, Engineering Failure Analysis, Vol. 35, 2013, pp. 95-103

[7] Bošnjak S., Petković Z., Atanasovska I., Milojević G., Mihajlović V.: Bucket chain excavator: Failure analysis and redesign of the counterweight boom supporting truss columns, Engineering Failure Analysis, Vol. 32, 2013, pp. 322-333

[8] Bošnjak S., Momčilović D., Petković Z., Pantelić M., Gnjatović N., Failure investigation of the bucket wheel excavator crawler chain link, Engineering Failure Analysis, Vol. 35, 2013, 462-469

[9] Bošnjak S., Arsić M., Gnjatović N., Milenović I., Arsić D., Failure of the bucket wheel excavator buckets, Engineering Failure Analysis, Vol. 84, 2018, pp. 247-261

[10] Petrović A., Maneski T., Trišović N., Ignjatović D., Dunjić M.: Identification of crack initiation cause in pylons construction of the excavator SchRs630, Technical Gazette, Vol. 25(2), 2018, pp. 486-491

[11] Petrović A., Ignjatović D., Sedmak S., Milošević-Mitić V., Momčilović N., Trišović N., Jeremić L., Model analysis of bucket wheel excavator SchRs 630 strength, Engineering Failure Analysis, Vol. 126, 2021, pp. 105451

[12] Kirin S., Sedmak A. Zaidi R., Grbović A., Šarkočević Ž.: Comparison of experimental, numerical and analytical risk assessment of oil drilling rig welded pipe based on fracture mechanics parameters, Engineering Failure Analysis, Vol. 114, 2020, 104600

[13] Hagarova M., Baranova G., Peterka P., Bulko B., Hrubovčakova M., Girman V.: Failure analysis of a gas pipeline at the kinked dent location with crack indications, Engineering Failure Analysis, Vol. 153, 2023, 107579

[14] Chen M.T., Chen Y., Young B.: Experimental investigation on cold-formed steel elliptical hollow section T-joints, Engineering Structures, Vol. 283, 2023, 115593

[15] Bonilla J., Mirambell E., Arrayago I.: Numerical analysis of curved steel plate girders subjected to patch loading, Engineering Structures, Vol. 297, 2023, 117015

[16] Amrous H., Yossef N. M., El-Boghdadi M. H.: Experimental study and structural analysis of tapered steel beams with cellular openings, Engineering Structures, Vol. 288, 2023, 116212

[17] Jimenez de Cisneros Fonfria J. J., Olmeda E., Sanz S., Garrosa M., Diaz V.: Failure analysis of a train coach underframe, Engineering Failure Analysis, Vol. 156, 2024, 107756

[18] Sitong W., Jinghua Z., Chao Z., Qing S.: Experimental and numerical investigation on the ultimate strength of multiple-ring-stiffened tube-gusset X-Joints under biaxial compressions, Engineering Structures, Vol. 289, 2023, 116308

[19] Wang K., Zhou X-H., Gao Y., Tan J-K., Wang G-Z., Wang Y-H.: Ultimate strength of CFST-gusset plate joints with ring stiffener plates under tension, Engineering Structures, Vol. 294, 2023, 116783

[20] Papatheocharis T., Plakias G., Zervaki A., Perdikaris P., Karamanos S.: Ultimate strength and fatigue of stiffened welded tubular joints in floating energy production structures, Engineering Structures, Vol. 297, 2023, 116985

[21] Pandey M., Young B.: Static performance and design of cold-formed high strength steel rectangular hollow section X-joints, Engineering Structures, Vol. 288, 2023, 114997

[22] Amraei M., Ahola A., Afkhami S., Björk T., Heidarpour A., Zhao X. L.: Effects of heat input on the mechanical properties of butt-welded high and ultra-high strength steels, Engineering Structures, Vol. 198, 2019, 109460

[23] Amraei M., Afkhami S., Javaheri V., Larkiola J., Skriko T., Björk T., Zhao X. L.: Mechanical properties and microstructural evaluation of the heat-affected zone in ultra-high strength steels, Thin-Walled Structures, Vol. 157, 2020, 107072

[24] Hemer A., Milović Lj., Grbović A., Aleksić B., Aleksić V.: Numerical determination and experimental validation of the fracture toughness of welded joints, Engineering Failure Analysis, Vol. 107, 2020, 104220

[25] Suvan Dev Choudhury, Waris Nawaz Khan, Zhe Lyu, Leijun Li: Failure analysis of blowholes in welded boiler water walls, Engineering Failure Analysis, Vol. 153, 2023, 107560

[26] Ghimire A., Wald F., Vild M., Kabelac J.: Numerical design calculation of the high-strength steel welds, Engineering Structures, Vol. 300, 2024, 117201

[27] Ramos H. M. E., Tavares S. M. O., de Castro P. M. S. T.: Numerical modelling of welded T-joint configurations using SYSWELD, Science and Technology of Materials, Vol. 30, Suppl. 1, 2018, pp. 6-15

[28] Németh, A., & Fischer, S. (2021) Investigation of the glued insulated rail joints applied to CWR tracks. Facta Universitatis, Series: Mechanical Engineering, 19(4), 681-704

[29] Fischer, S., Harangozó, D., Németh, D., Kocsis, B., Sysyn, M., Kurhan, D., & Brautigam, A. (2023) Investigation of heat-affected zones of thermite rail welding. Facta Universitatis, Series: Mechanical Engineering. https://doi.org/10.22190/FUME221217008F

[30] Brautigam, A., Szalai, S., & Fischer, S. (2023) Investigation of the application of austenitic filler metals in paved tracks for the repair of the running surface defects of rails considering field tests. Facta Universitatis, Series: Mechanical Engineering, https://doi.org/10.22190/FUME230828032B

[31] Barna, V., Brautigam, A., Kocsis, B., Harangozó, D., & Fischer, S. (2022) Investigation of the effects of Thermit welding on the mechanical properties of the rails. Acta Polytechnica Hungarica, 19(3), 37-49, https://doi.org/10.12700/APH.19.3.2022.3.4

[32] Ézsiás, L., Tompa, R., & Fischer, S. (2024) Investigation of the possible correlations between specific characteristics of crushed stone aggregates. Spectrum of Mechanical Engineering and Operational Research, 1(1), 10-26, https://doi.org/10.31181/smeor1120242

[33] Bubbico R.: A statistical analysis of causes and consequences of the release of hazardous materials from pipelines. The influence of layout, Journal of Loss Prevention in the Process Industries, Vol. 56, 2018, pp. 458-466

[34] Woldesellasse H., Tesfamariam S.: Risk analysis of onshore oil and gas pipelines: Literature review and bibliometric analysis, Journal of Infrastructure Intelligence and Resilience, Vol. 2, Issue 4, 2023, 100052

[35] Arandjelovic M., Djordjevic B., Sedmak S., Radu D., Petrovic A., Dikic S., Sedmak A.: Failure analysis of welded joint with multiple defects by extended Finite Element Method and Engineering Critical Analysis, Engineering Failure Analysis, Vol. 160, 2024, 108176

[36] Mitrović N., Mitrović A., Travica M.: Tensile testing of flat thin specimens using the two-dimensional digital image correlation method, Structural Integrity And Life Vol. 23(1), 2023, pp. 9-13

[37] Aranđelović M., Petrović A., Sedmak S.: Digital image correlation application to structural integrity assessment, Structural Integrity And Life, Vol. 24(1), 2024, pp. 87-91

[38] Szalai, S., Fehér, V., Kurhan, D., Németh, A., Sysyn, M., & Fischer, S. (2023) Optimization of surface cleaning and painting methods for DIC measurements on automotive and railway aluminum materials. Infrastructures, 8(2), 27, https://doi.org/10.3390/infrastructures8020027

[39] Koch E., Ray R. P.: Impact Assessment of Railway Bridge Construction Schedule, based on 3D Geotechnical Finite Element Modeling, Acta Polytechnica Hungarica, Vol. 21, No. 1, 2024, pp 187-205

[40] Hamed Elmoghazy Y., Safaei B., Sahmani S.: Finite Element Analysis for Dynamic Response of Viscoelastic Sandwiched Structures Integrated with Aluminum Sheets, Vol. 21(4), 2023, pp. 591-614

[41] Sedmak A., Grbović A., Zaidi R., Kirin S., Vitas N., Golubović T., Vučetić I.: Numerical, Analytical and Experimental Determination of Remaining Life of A Pipe With an Axial Crack, Structural Integrity and Life, Vol. 23(3), 2023, pp. 239-244